35. ALTERATION OF REMNANT ARC DEBRIS, SITE 448, PALAU-KYUSHU RIDGE, PHILIPPINE SEA, DEEP SEA DRILLING PROJECT LEG 59

Jeffrey B. Aldrich,[1] Thomas T. Tieh, and Robert B. Scott, Texas A&M University, College Station, Texas

INTRODUCTION

Alteration in a submarine remnant volcanic arc should leave an important record of (1) the mineralogy of sea water–volcanic arc rock interaction; (2) the chemistry of solid reaction products; (3) the isotopic characteristics of such reactions (Muehlenbachs and Clayton, 1972; Spooner, Beckinsale, et al., 1977; Spooner, Chapman, et al., 1977); (4) the metallogenesis within such a sequence (Mitchell and Bell, 1973); and (5) the geothermal gradient during the alteration. The volcaniclastic breccias, tuffs, and igneous units of Sites 448 (993 m) and 451 (930.5 m) on the Palau-Kyushu and West Mariana ridges, respectively, are particularly suited for such studies because the thick sequences have remained submarine throughout their history, seemingly unaffected by magmatic or hydrothermal events after cessation of volcanic activity. Also, shipboard observations indicated a change in alteration products with depth. At both sites the igneous units and volcaniclastic rocks were altered to brownish clays and zeolites near the top of the volcanic sequence; to bright blue green clays and zeolites at moderate depths; and to very dark, nearly opaque, forest green clays and zeolites at still greater depths. Native copper occurs both as disseminated pockets in the volcaniclastic breccias and vesicular basalts and as veins in the breccias; native copper is restricted to stratigraphic levels characterized by the absence of sulfides or oxides of copper and iron. Although some native copper is found in vesicles of basalts and may be orthomagmatic, most of it is clearly secondary. Near dikes and sills, higher sulfur fugacity conditions caused the precipitation of iron and copper sulfides with an absence of native copper (Garrels and Christ, 1965). The occurrence of native copper may be an initial stage of Cu metallogenesis that forms porphyry coppers in island arcs (Mitchell and Bell, 1973). This study will address primarily the possibility that hydrothermal sea water interaction with volcanic arc rocks has created the mineralogical and isotopic zonation in Leg 59 cores. Hydrothermal activity can be expected in a rapidly growing island arc and is probably the result of a high geothermal gradient prevalent during arc magmatic activity. The chemical character of the alteration is further discussed by Hajash (this volume).

PROCEDURES

All zeolite identification was accomplished by powder camera diffraction, using 114.59-mm powder cameras with monochromatic CuK_α radiation. Zeolite crystals, located under a binocular microscope, were either handpicked before grinding or crushed *in situ*. The powders were then mounted on a glass fiber with vaseline for powder camera diffraction. The methods for clay identification were those outlined by DiStefano (1978), using a Philips X-ray diffractometer with CuK_α radiation and a $1° \; 2\theta$ per minute scanning rate. Whole-rock samples were disaggregated in a ball mill, then dispersed in a Na_2CO_3 solution with a pH of 10. The 2-μm clay fraction was separated by a centrifuge and then rinsed three times with distilled water. Smear slides of untreated clays, Mg-saturated clays, and K-saturated clays were prepared for each clay sample. The Mg-saturated slide was allowed to equilibrate in an ethylene glycol atmosphere to test for expandable clay minerals. Diffractograms were subsequently obtained from the untreated and treated samples. In order to identify expandable clays and to distinguish the chlorite from the kaolinite peaks, two diffractograms were obtained for each smear slide—the first after all samples had been heated to 350°C for one hour and the second after heating to 550°C for an additional hour.

Oxygen isotope studies on ground whole rock and untreated clay fractions were done by K. Muehlenbachs and R. Houghton, using the BrF_5 method (Clayton and Mayeda, 1963). Atomic absorption spectrophotometric analyses for Cu were made on whole-rock samples of the igneous units and several volcaniclastic units.

RESULTS

Samples of volcaniclastic rocks and igneous units from Site 448 (Holes 448 and 448A) show extensive alteration of matrix material and phenocrysts to clays and the growth of zeolites and clays in vesicles, veins, and grain interstices (for details, see Petrographic Descriptions). Although all units show extensive alteration, the volcaniclastic breccias are by far the most altered. Only glass rims of pillow lavas near the top of the volcanic sequence are unaltered (Scott, this volume). Tables 1 and 2 show preliminary results of mineralogical and isotopic studies. Phillipsite, a K- and Ca-rich zeolite, is the most abundant zeolite to depths of 584 meters and is present in all rock types. From 548 to 717 meters, this zeolite is still abundant in volcaniclastic breccias but competes with Fe-, Mg-, and Na-rich alteration products. At the deeper levels, basaltic flows contain no phillipsite. From 717 meters sub-bottom to the bottom of the hole, the Fe-, Mg-, and Na-rich alteration products—primarily nontronite, actinolite, natrolite, and a distinctive, new clay mineral—are abundant and occur in all rock types. This last clay, which occurs below 664 meters sub-bottom, is a smectite-vermiculite-chlorite (SVC) mixed-layer silicate that appears as a well-crystallized clay mineral; the only sample showing poor crystallinity is at

---

[1] Present address: Pennzoil Company, P.O. Box 2967, Houston, Texas.

Table 1. Mineralogical and isotopic composition of alteration products in samples from DSDP Hole 448.

Core/Section/ Interval (cm)/Piece	Sub-bottom Depth (m)	Clays Identified	Zeolites Identified	Carbonate	Other Secondary Minerals	$\delta^{18}O$ (SMOW) Whole Rock (‰)	Clays (‰)
37-1 (51–53)	338.0	saponite, kaolinite					
43-2 (20–22)	377.2	smectite					
46-1 (100–103)	405.0	smectite	phillipsite	calcite			
47-2 (21–24), 3	415.2	kaolinite	phillipsite				
48-1 (118–120)	424.2		phillipsite	calcite			
50-2 (50–57), 1I	444.0	celadonite, kaolinite	phillipsite	calcite			
50-3 (111–116)	446.1	kaolinite	phillipsite	calcite	native copper		
51-1 (108–110)	452.6		phillipsite	calcite			
53-1 (0–3), 1A	470.5		phillipsite	calcite			
53-2 (56–61), 1J	472.5		phillipsite & chabazite				
55-1 (108–116), 9E	490.6	chlorite	phillipsite? chabazite	calcite	native copper		
57-1 (30–36), 2C	508.8	kaolinite	acicular & platy zeolites	calcite	native copper Fe oxide		
57-2 (10–22), 1B	510.1	kaolinite	platy zeolite	calcite			
58-2 (47–51), 1L	520.0		phillipsite	calcite	native copper		
58-3 (112–115), 3Q	522.1	kaolinite	phillipsite				
59-1 (61–63), 3B	528.1	smectite	phillipsite				
59-3 (49–53), 5A	531.0	brown smectite, kaolinite					

Note: Blanks under carbonate and other secondary mineral columns indicate an absence of that mineral group. Blanks under the clay, zeolite, and $\delta^{18}O$ columns indicate that no analysis was made.

Table 2. Mineralogical and isotopic composition of alteration products in samples from DSDP Hole 448A.

Core/Section/ Interval (cm)/Piece	Sub-bottom Depth (m)	Clays Identified	Zeolites Identified	Carbonate	Other Secondary Minerals	$\delta^{18}O$ (SMOW) Whole Rock (‰)	Clays (‰)
15-1 (29–31), 1E	527.8	kaolinite				19.0	24.2
16-2 (68–75), 6E	539.2	kaolinite, chlorite	phillipsite, chabazite				
18-1 (110–114), 8H	550.6		extensive				
21-1 (53–59), 5A	575.6	smectite	phillipsite				
21-1 (76–80), 5F	575.8	smectite	phillipsite				
22-1 (5–11), 1B	584.6	kaolinite, chlorite					
22-1 (22–27), 1E	584.7	kaolinite, chlorite	natrolite, phillipsite			9.2 altered rock 9.1 unaltered glass	24.7
29-1 (31–34)	632.3	green smectite		calcite			
33-1 (131–138), 5B	664.9	SVC, nontronite, chlorite, illite			native copper		
36-3 (61–69)	692.6	green smectite	natrolite, phillipsite	calcite			
38-1 (96–103), 8A	709.0	clay, chlorite (SVC?)		calcite	actinolite	10.5	20.0
40-1 (30–37), 4	717.8	chlorite-rich clay	natrolite, phillipsite				
41-1 (89–91)	727.9	SVC					
44-1 (22–47)	755.8	SVC					
44-1 (67–71)	756.2	Gray blue	analcime		pyrite		
45-2 (12–14)	766.6	smectite, SVC					
46-1 (65–75), 4B	768.7	SVC	stilbite		tremolite		
57-2 (90–95), 6B	848.9	SVC, chlorite			actinolite, leucoxene	7.7	11.1
58-2 (47–51), 1L	857.5		chabazite, natrolite(?)				
66-2 (122–129)	913.3	SVC, kaolinite					

Note: Blanks under carbonate and other secondary mineral columns indicate an absence of that mineral group. Blanks under the clay, zeolite, and $\delta^{18}O$ columns indicate that no analysis was made.

664 meters. Above this level, SVC is not identified. It is thought that the smectite in the SVC might be saponite, but this has not been confirmed (DiStefano, 1978). Kaolinite is the dominant clay at the top of the volcanic section and is present as a major alteration phase downhole to about 699 meters sub-bottom. Although high abundances of kaolinite are restricted to the upper part of the section, it has also been identified in the deepest sample (914 m sub-bottom) coexisting with SVC.

The $\delta^{18}O$ values of clays decrease from 24.2 ‰ at 527.8 meters to 11.1 ‰ at 849 meters. Whole rocks show a similar decrease from 19.0 ‰ at 527.8 meters to 7.17 ‰ at 849 meters.

Petrographic descriptions of the alteration are given in the following samples with thin sections available for study, and photomicrographs and scanning electron microscope photographs have been described in Plate 1, Figures 1 through 4.

PETROGRAPHIC DESCRIPTION[2]

448-47-2 (21–24), 3: Aphanitic, vesicular pillow basalt contains glass. Vesicles are less than 15% of the rock and are ½ to 1 mm in diameter. Most vesicles are filled with phillipsite, and the glass is altered to dark yellowish orange (10 YR 6/6) clay.

448-50-2 (50–57), 1I: Volcaniclastic breccia contains clasts of aphanitic basalt, and quartz diorite. Clast size up to 2 cm. Matrix consists of ash altered to pale grayish olive (10 Y 5/2) clay, and clasts are altered to dark yellowish orange (10 YR 6/6) clay. No carbonates but some zeolite veins are present.

448-53-1 (0–3), 1A: Aphanitic, vesicular pillow basalt has glass present. Vesicles are about 5% of the rock and ½ mm in diameter. Most vesicles are lined or filled with phillipsite, and glass is altered to dark yellow orange (10 YR 6/6) clay.

448-53-2 (56–61), 1J: Aphanitic, vesicular pillow basalt with no glass. Vesicles are about 5% of the rock and up to 1 mm in diameter. Groundmass shows an alteration to fine clays. Globular growth of cubic crystals of chabazite on euhedral phillipsite occur. Phillipsite-filled veins are common.

448-55-1 (108–116), 9E: Volcaniclastic breccia consists of clasts of basalts with vesicles from 10 to 20% of the rock, glass, and pumice. Clast size is up to 5 mm in diameter. Matrix is moderate greenish yellow (10 Y 7/4) clay. Some vesicles of pumice clasts are filled with moderate yellow (5 Y 7/6) clay, and vesicles of basalts are filled with calcite and zeolites.

448-57-1 (30–36), 2C: Aphanitic, vesicular pillow basalt has no glass. Vesicles are about 5% of the volume and are up to 1 mm in diameter. Groundmass shows Fe oxide stains ½ to 2 mm in diameter. Most vesicles are filled with calcite.

448-57-2 (10–22), 1B: Aphanitic, vesicular pillow basalt has no glass. Vesicles are about 5% of the volume and up to 1 mm in diameter. Vesicles are filled with calcite over zeolites, and there are several calcite-filled veins from 1 to 10 mm wide.

448-58-2 (47–51), 1L: Volcaniclastic breccia with clasts of basalts, andesite, pumice, and glass. Matrix is altered to grayish yellow (5 Y 8/4) clay, and glass is altered to moderate yellow (5 Y 7/6) clay. Basalt clasts have 20 to 30% vesicles less than 1 to 5 mm in diameter and 10% vesicles 2 mm in diameter. Vesicles are lined with phillipsite, and clasts are split by calcite-filled fractures. Olivine, pyroxene, and plagioclase are altered and in some cases totally replaced by carbonates and zeolites. Abundant zeolites fill large cavities.

448-58-3 (112–115), 3Q: Vesicular basalt contains altered plagioclase phenocrysts of 1 to 2 mm. Vesicles are 15 to 20% of the rock and 1 to 3 mm in diameter. Groundmass shows a hyalopilitic texture, and vesicles are lined with phillipsite. Plate 1, Figs. 3 and 4 show similar vesicle mineralization.

448-59-1 (61–63), 3B: Vesicular basalt with altered plagioclase phenocrysts of 1 to 2 mm. Vesicles are 15 to 20% of the rock and 1 to 3 mm in diameter. Groundmass extremely altered to very grayish yellow (5 Y 9/4) clays. Vesicles lined with zeolite with no evidence of carbonate.

448A-15-1 (29–31), 1E: Basalt flow contains altered plagioclase, clinopyroxene, orthopyroxene, and olivine phenocrysts less than 1 mm in diameter. Glass is altered to pale yellowish orange (10 YR 8/6) clay. Vesicles and small fractures are filled with zeolite.

448A-16-2 (68–75), 6E: Vesicular pillow basalt has a glass rim. Vesicles are 15 to 35% of the rock and ¼ to 2 mm in diameter. Alteration of glass to pale yellowish orange (10 YR 8/6) clay. Vesicles are lined with zeolites. No carbonates are present.

448A-21-1 (53–59), 5A: Volcaniclastic breccia with clasts of plagioclase and clinopyroxene basalt. Matrix has been altered to grayish, yellow green (5 6Y 7/2) clay. Vesicles in basalts are lined with zeolites or smectites.

448A-22-1 (22–27): Volcaniclastic breccia with clast of basalt, pumice, and vitrophyre. Clasts are up to 4 mm in diameter, and matrix exhibits flow banding. Vesicles in basalt are filled with platy and acicular zeolites.

448A-33-1 (131–138) 5B: Aphanitic basalt contains microphenocrysts of plagioclase and an extremely altered groundmass. Thin veins containing native copper are present. Chlorite is abundant.

448A-40-1 (30–37), 4: Aphanitic basalt contains microphenocrysts of plagioclase and a groundmass altered to dusty olive green (5 6Y 4/2) clays. Zeolites are extensive throughout the rock.

448A-46-1 (65–75), 4B: Volcaniclastic breccia consists of clasts of coarse tuff and extremely altered basalt. Matrix and vesicles contain acicular stilbite and carbonates (Plate 1, Fig. 2).

448A-57-2 (90–95), 6B: Volcaniclastic breccia contains clasts of basalt, glassy tuff aggregates of fragments of vitrophyres and devitrified glass. All fragments show an orbicular texture and have variable mineralogies. Some contain actinolite, others have chlorite, and still others contain leucoxene.

CONCLUSIONS

The nature and degree of alteration of the volcaniclastic breccias and flows recovered at Site 448 vary with depth, as evidenced by the alteration product mineralogy and the oxygen isotopic stratigraphy of the alteration products (Tables 1 and 2). These alteration products exhibit a chemical trend of K- and Ca-rich phases in the upper part of the cores, giving way to Fe-, Mg-, and Na-rich phases in the lower part. This trend is expected for the transition from ambient sea water or low-temperature alteration at shallow depths to hydrothermal alteration at greater depths (Tomasson and Kristmannsdottir, 1972; Bischoff and Dickson, 1975; Hajash, 1975; Scott and Hajash, 1976). In an analogous core, in Hole 296 in the northern extension of the Palau-Kyushu Ridge, Donnelly (1975) reported finding phillipsite in the upper units of Hole 296, as in the upper section at Site 448; also, shipboard studies of Hole 296 reported a dark clay-serpentine alteration product in the lower units similar to that at Site 448 (Karig, Ingle, et al., 1975). Other investigations reporting trends similar to those at Site 448 include the zeolite zonation in eastern Iceland by Walker (1960) and the hydrothermal facies of Burnham (1962).

The occurrence of native copper veinlets and blebs indicates that copper and perhaps other metals have been affected by secondary distribution processes such as hydrothermal fluids. Analyses for Cu and major elements were routinely made by atomic absorption in order to study volcanic unit chemistry (Scott, this volume), but only a few volcaniclastic breccias were analyzed, near the top of the section. Nevertheless, several observations are worth noting: The average of the thick, uppermost flow units (6–14) is 160 ppm Cu; of the lower volcanic units (16–43), 100 ppm; of intrusive units, 133; and of volcaniclastic breccias, 102 ppm Cu. These values are somewhat higher than those reported for arc tholeiites (Gill, 1970; Ewart and Bryan, 1972; Brown et al., 1977) but may be characteristic of this particular arc. The irregularities in copper abundance (Table 3) may be due to copper redistribution over large portions of the core rather than to locality—

---

[2] Numbers in parentheses indicate intervals in cm; numeral and numeral followed by letter indicate piece.

Table 3. Copper abundances in DSDP Holes 448 and 448A.

Core/Section/Interval Center (cm)	Unit	Rock	Cu (ppm)
Hole 448			
37-1-52	6	basalt flow	220
39-1-75	6	basalt flow	193
40-1-68	6	basalt flow	105
43-2-21	8	basalt flow	125
47-2-22	9	basalt flow	137
48-1-119	9	basalt flow	145
48-2-18	9	basalt flow	151
50-2-51	10	volcaniclastic breccia	158
50-3-80	10	volcaniclastic breccia	83
50-4-50	10	volcaniclastic breccia	73
53-1-2	11	basalt flow	136
53-2-58	11	basalt flow	163
55-1-110	12	volcaniclastic breccia	104
57-1-33	12	volcaniclastic breccia	168
58-2-48	12	volcaniclastic breccia	79
58-2-50	12	volcaniclastic breccia	78
58-3-113	13	basalt flow	182
59-1-62	13	basalt flow	161
59-3-51	13	basalt flow	140
Hole 448A			
15-1-30	13	basalt flow	183
16-2-71	13	basalt flow	156
18-1-111	14	basalt flow	240
18-2-113	14	basalt flow	184
21-1-56	15	volcaniclastic breccia	129
21-1-77	15	volcaniclastic breccia	61
22-1-7	15	volcaniclastic breccia	31
26-2-32	16	basalt flow	44
28-1-96	18	basalt flow	48
33-1-134	20	basalt flow	41
33-2-6	20	basalt flow	45
36-5-53	22	basalt flow	114
37-2-141	23	basalt flow	>466
38-1-99	23	basalt flow	51
40-1-33	24	basalt flow	119
41-1-90	26	basalt dike	39
41-2-12	27	basalt dike	>464
41-4-16	27	basalt dike	100
44-1-34	31	basalt flow	156
45-1-43	31	basalt flow	174
45-2-13	31	basalt flow	122
46-1-65	32	volcaniclastic breccia	161
47-1-71	33	basalt sill	125
47-1-73	33	basalt sill	192
47-3-130	33	basalt sill	126
47-3-140	33	basalt sill	160
50-1-47	35	basalt sill	158
50-1-95	35	basalt sill	149
50-1-99	35	basalt sill	145
51-1-84	37	basalt dike	186
51-1-86	37	basalt dike	178
51-3-135	37	basalt dike	119
52-2-126	39	basalt flow	130
52-2-130	39	basalt flow	166
54-3-81	41	basalt flow	134
56-1-31	41	basalt flow	135
57-1-96	43	basalt flow	15
59-2-126	47	basalt sill	144
62-1-58	49	basalt dike	123
62-1-61	49	basalt dike	198
62-2-3	49	basalt dike	89
62-2-10	49	basalt dike	115
65-2-128	51	basalt dike	67
65-2-132	51	basalt dike	191
66-2-123	51	basalt dike	101
66-2-127	51	basalt dike	108

Note: The basalts are arc tholeiites (Scott, this volume). The unit numbers are those used in the Site 448 report, this volume.

for example, in Hole 448A, between Cores 21 and 41, where the Cu values are less than 68 ppm, excluding two copper spikes. However, if the two spikes of copper in Units 23 and 27 are included, the copper content average is essentially equal to that of the rest of the core. Therefore, no overall removal or addition of copper is indicated, and a simple case for redistribution can be made. A comparison of shipboard observations of native copper and pyrite mineralization (Table 4) with the copper analyses of Table 3 shows little correlation except with Unit 23. This mismatch suggests that a sampling problem exists: High concentrations of copper are very local and difficult to record analytically with only a few random samples. Table 4 also shows a vertical zonation of mineralization from highly localized copper veins in volcaniclastic breccia (Units 16, 20, and 23) to disseminated pyrite in volcaniclastic breccias and flows (Units 30, 32, 46, and 51).

Oxygen isotope data on the clay alteration products show a decrease in $\delta^{18}O$ values of 13.1 ‰ from 537 meters to 846 meters. Muehlenbachs (personal communication) has suggested the clay $\delta^{18}O$ value of 11.1 ‰ in Sample 448A-57-2, 90–95 cm, 6B (Table 1) may indicate a temperature as high as 170°C but is more likely to indicate temperatures in the range of 120°C. This sample was taken from a volcaniclastic breccia 10 meters above a basaltic sill. If this $\delta^{18}O$ value is not the product of local heating by the sill, the range of 120° to 170°C would indicate geothermal gradients approximately six to nine times the normal continental geothermal gradient. Obviously, a high geothermal gradient is expected in a submerged active magmatic arc because of abundant igneous activity in the vicinity.

Studies by Migdisov et al. (this volume) on the isotopic character of carbonate veins and coatings in the volcaniclastic breccias of Holes 448 and 448A contrast with this conclusion; they find little isotopic evidence to

Table 4. Copper and pyrite mineralization, DSDP Holes 448 and 448A.

Core/Section/Interval Center (cm)	Unit	Rock	Mineralization
Hole 448			
50-2, 150	10	volcaniclastic breccia	copper veins
50-3, 115	10	volcaniclastic breccia	copper veins
55-1, 110	12	volcaniclastic breccia	copper veins
56-1, 80	12	volcaniclastic breccia	copper veins
56-1, 87	12	volcaniclastic breccia	copper veins
56-1, 35	12	volcaniclastic breccia	copper veins
Hole 448A[a]			
26-2	16	basalt flow	disseminated Cu
32-1	20	basalt flow	disseminated Cu
33-1	20	basalt flow	disseminated Cu
33-2	20	basalt flow	disseminated Cu
37-3	23	basalt flow	disseminated Cu
44-1	30	volcaniclastic breccia	disseminated pyrite
44-2	30	volcaniclastic breccia	disseminated pyrite
46-1	32	volcaniclastic breccia	disseminated pyrite
59-3	46	volcaniclastic breccia	disseminated pyrite
66-1	51	basalt flow	disseminated pyrite

[a] No interval is indicated for sections with mineralization throughout the core.

support an abnormally high geothermal gradient. We suggest that the silicates became isotopically fixed at the time of their formation, during the active arc portion of Palau-Kyushu evolution, when the geothermal gradient was high; only after inactivity during the remnant arc stage and return of the volcanic debris to a lower geothermal gradient did the carbonates become isotopically fixed. To be sure, this is only a suggestion, and much more detailed mineralogical, isotopic, and chemical work should be done on the cores from both Sites 448 and 451 (West Mariana Ridge) to identify the thermal state evolution and metallogenesis of arcs in their initial stages of evolution.

ACKNOWLEDGMENTS

This chapter is Texas A&M University Geodynamics Research Program Contribution Number 12.

REFERENCES

Bischoff, J. L., and Dickson, F. W., 1975. Seawater-basalt interaction at 200°C and 500 bars: Implications for origin of sea floor heavy-metal deposits and regulation of seawater chemistry. *Earth Planet. Sci. Lett.*, 25:385–387.

Brown, G. M., Sigurdsson, H., Tomblin, J. F., and Arculus, R. J., 1977. Geochemistry of the Lesser Antilles volcanic island arc. *Geochim. Cosmochim. Acta*, 41:785–801.

Burnham, C. W., 1962. Facies and types of hydrothermal alteration. *Econom. Geol.*, 57:768–784.

Clayton, R. N., and Mayeda, T. K., 1963. The use of bromine pentafluoride in the extraction of oxygen from oxides and silicates for isotopic analysis. *Geochim. Cosmochim. Acta*, 27:43–52.

DiStefano, M., 1978. Diagenetic alteration of volcanic rock fragments in the Stevens sandstone, San Joaquin Basin, California. [Ph.D. dissert.]. Texas A&M University.

Donnelly, T. W., 1975. Neogene explosive volcanic activity of the western Pacific: Sites 292 and 296, DSDP Leg 31. *In* Karig, D. E., Ingle, J.C., Jr. et al., *Init. Repts. DSDP*, 31: Washington (U.S. Govt. Printing Office), 577–598.

Ewart, A., and Bryan, W. B., 1972. Petrography and geochemistry of the igneous rocks from Eva, Tonga Islands. *Geol. Soc. Am. Bull.*, 83:3281–3298.

Garrels, R. M., and Christ, C. L., 1965. *Solutions, Minerals and Equilibria:* San Francisco (Freeman, Cooper and Co.).

Gill, J. B., 1970. Geochemistry of Viti Levu, Fiji and its evolution as an island arc. *Contr. Mineral. Petrol.*, 27:179–203.

Hajash, A., 1975. Hydrothermal processes along mid-ocean ridges: An experimental investigation. *Contr. Mineral. Petrol.*, 53: 205–226.

Karig, D. E., and Ingle, J. C., Jr., et al., 1975. *Init. Repts. DSDP*, 31: Washington (U.S. Govt. Printing Office).

Mitchell, A. H., and Bell, J. D., 1973. Island-arc evolution and related mineral deposits. *J. Geol.*, 81:381–405.

Muehlenbachs, K., and Clayton, R. N., 1972. Oxygen isotope geochemistry of submarine greenstones. *Can. J. Earth Sci.*, 9:471–478.

Scott, R. B., and Hajash, A., 1976. Initial submarine alteration of basaltic pillow lavas. *Am. J. Sci.*, 276:480–501.

Spooner, E. T. C., Beckinsale, R. D., England, P. C. et al., 1977. Hydration, $\delta^{18}O$ enrichment and oxidation during ocean floor hydrothermal metamorphism of ophiolitic metabasic rocks from East Liguria, Italy. *Geochim. Cosmochim. Acta*, 41:857–871.

Spooner, E. T. C., Chapman, H. T., and Snewing, J. D., 1977. Strontium isotopic contamination and oxidation during ocean floor hydrothermal metamorphism of the ophiolitic rocks of the Troodos Massif, Cyprus. *Geochim. Cosmochim. Acta*, 41:873–890.

Tomasson, J., and Kristmanndottir, H., 1972. High temperature alteration minerals and thermal brines, Reykjanes, Iceland. *Contr. Mineral. Petrol.*, 36:123–134.

Walker, G. P. L., 1960. Zeolite zones and dike distribution in relation to the structure of the basalts of Eastern Iceland. *J. Geol.*, 68:515–528.

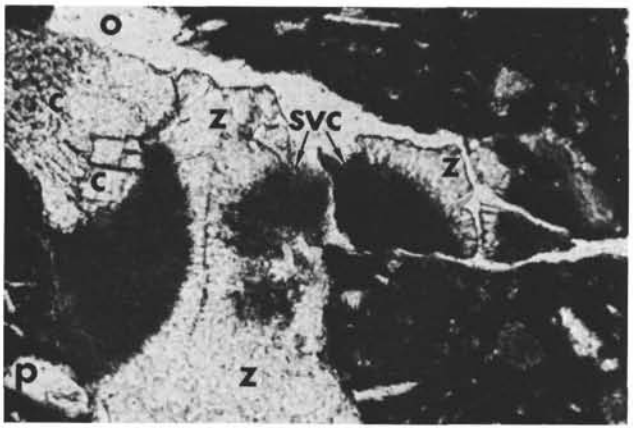

1

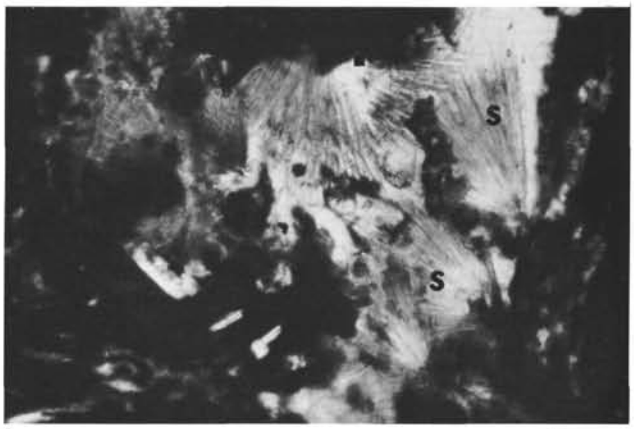

2

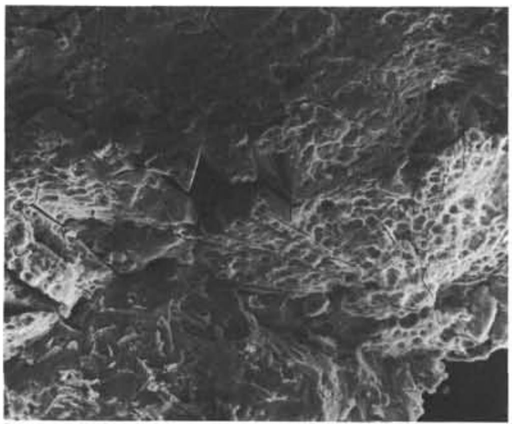

3

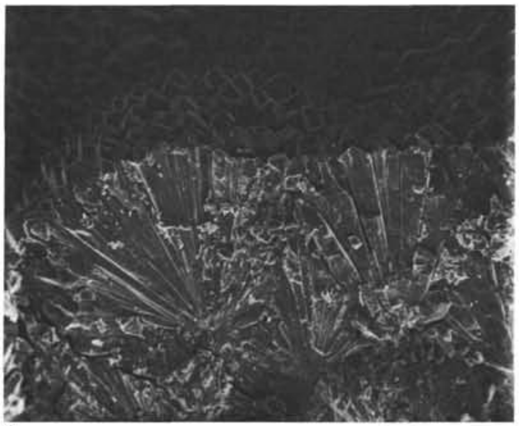

4

Plate 1. Photomicrographs and scanning electron microscope (SEM) photographs of altered volcaniclastic material.

Figure 1. Sample 448A-38-1 (96–103 cm), Piece 8A. Photomicrograph of a devitrified basalt vitrophyre with fractures filled with alteration minerals. (Z = isotopic zeolites, C = calcite, P = plagioclase, SVC = a mixed clay-chlorite with radiating needles of actinolite, O = open; bar scale = 0.1 mm; plane polarized light.)

Figure 2. Sample 448A-46-1 (65–75 cm). Photomicrograph of a volcaniclastic breccia with extreme hydrothermal alteration. Acicular growths of stilbite(?) in clast interstices. (S = stilbite; bar scale = 0.1 mm; plane polarized light.

Figure 3. Sample 448-46-1 (100–103 cm). SEM photograph of phillipsite that has undergone dissolution representing at least a two-stage alteration process. This sample comes from a vesicular pillow basalt ($\times 10^2$).

Figure 4. Sample 448-58-2 (47–51 cm), Piece 1L. SEM photograph of phillipsite clusters lining a vesicle of a basalt clast in a volcaniclastic breccia (×230).